GPR applications in mapping the subsurface root system of street trees with road safety-critical implications

This is the Accepted Version of the final output.

UWL repository link: https://repository.uwl.ac.uk/id/eprint/4379/

Alternative formats: If you require this document in an alternative format, please contact:
open.research@uwl.ac.uk

GPR applications in mapping the subsurface root system of street trees with road safety-critical implications

F. Tosti[1]   L. Bianchini Ciampoli[2]   M.G. Brancadoro[1]   A.M. Alani[1]

[1]*School of Computing and Engineering, University of West London (UWL),*
St Mary's Road, Ealing, London W5 5RF, UK
email: Fabio.Tosti@uwl.ac.uk; 21358807@student.uwl.ac.uk; Amir.Alani@uwl.ac.uk
[2]*Department of Engineering, Roma Tre University, Via Vito Volterra 62, 00146, Rome, Italy*
email: luca.bianchiniciampoli@uniroma3.it

Abstract

Street trees are an essential element of urban life. They contribute to the social, economic and environmental development of the community and they form an integral landscaping, cultural and functional element of the infrastructure asset. However, the increasing urbanisation and the lack of resources and methodologies for the sustainable management of road infrastructures are leading to an uncontrolled growth of roots. This occurrence can cause substantial and progressive pavement damage such as cracking and uplifting of pavement surfaces and kerbing, thereby creating potential hazards for drivers, cyclists and pedestrians. In addition, neglecting the decay of the principal roots may cause a tree to fall down with dramatic consequences. Within this context, the use of the ground-penetrating radar (GPR) non-destructive testing (NDT) method ensures a non-intrusive and cost-effective (low acquisition time and use of operators) assessment and monitoring of the subsurface anomalies and decays with minimum disturbance to traffic. This allows to plan strategic maintenance or repairing actions in order to prevent further worsening and, hence, road safety issues. This study reports a demonstration of the GPR potential in mapping the subsurface roots of street trees. To this purpose, the soil around a 70-year-old fir tree was investigated. A ground-coupled GPR system with central frequency antennas of 600 MHz and 1600 MHz was used for testing purposes. A pilot data processing methodology based on the conversion of the collected GPR data (600 MHz central frequency) from Cartesian to polar coordinates and the cross-match of information from several data visualisation modes have proven to identify effectively the three-dimensional path of tree roots.

Keywords – street trees, tree roots detection, ground-penetrating radar (GPR), pavement damage, road safety

1. Introduction

Street trees are fundamental elements that provide social, economic and environmental benefits to urban areas [1-3]. It has been proven that greenspaces are beneficial for a community's wellbeing in urban environments as they ease social interactions between residents [4], increase the awareness of being part of a larger community and they may contribute to lower crime actions [5]. Street trees can also provide contribution to reduce stormwater runoff and energy consumption, improving the quality of air and increasing biodiversity [6, 7].

Mullaney et al. [3] showed that the overall economic benefits brought by street trees overcome the negatives by at least a factor of two. In this regard, negatives are primarily related to financial

costs for the damage caused by the uncontrolled growth of tree roots. These costs are allocated for maintenance purposes, repair and replacement of pavements [8], injury compensations, loss and replacement of street trees [9-11].

There exists an extensive literature on the interference between tree roots and road pavements and sidewalks, in terms of mechanisms of development and strategies of prevention, maintenance and repairing of the damage [12-16].

The damage is primarily due to the growing roots that displace the neighboring soil and cause cracking and uplifting of the pavement surface and kerbing. In fact, a natural vertical deep proliferation of the roots' path of a tree requires a porous soil, whereas most road infrastructures are built using a load-bearing base layer of compacted bound aggregates. To this effect, the compaction reduces the air voids in the soil and may contrast the vertical development of roots. Consequently, tree roots tend to expand radially and at shallower depths, thereby causing damage and unevenness of the pavement surface [17]. In addition, Wagar and Barker [12] reported that the hydrophilic roots proliferating at the condensed water zones underneath the asphalt layer are another major cause of asphalt cracking.

As a preventive countermeasure to reduce the risk of damage associated to uncontrolled tree roots growth, the use of permeable pavements has proven to favour the growth of roots at higher depths, where the moisture levels are more stable and homogeneous [3]. In addition, root barriers [10, 19] and structural soils [19] are used to manage a more controlled growth of roots.

Although street trees are an integral element of urban life, it is worth mentioning the hazard brought by unevenness and cracking of the pavement surface for people driving motor vehicles, cyclists and pedestrians. In addition, neglecting decay of the principal roots may cause a tree to fall down with dramatic consequences.

Extensive literature studies have proven relationships between traffic accidents and damage such as cracks, ruts and spalls [20-22], all of which can be related – inter alia – to tree roots uplifting from the underneath toward the asphalt surface.

The lateral location of damages on the carriageway makes these often disregarded by the highway administrators, mostly at the early stage of development, as the driving safety implications affecting cars and heavy vehicles may be negligible at this stage. Therefore, such a negligence lets the damage to further develop and, hence, it causes higher rehabilitation cost if the intervention is carried out at more belated stages.

In addition, it is also worth mentioning the safety concerns that inevitably involve cyclists and bikers. In this regard, trajectories of these road users are typically at the edge of the lateral lane or at the verges; hence, they collide mostly with the asphalt damage due to the uplifting of tree roots (Figure 1). Safe driving conditions could be then compromised by even slight uplifts of the asphalt surface and surface damage that may cause sudden deviations of trajectory with tremendous consequences [23, 24].

Within this context, an early-stage assessment and monitoring of the subsurface anomalies and decays would allow to plan strategic maintenance or repairing actions in order to prevent further worsening and, hence, road safety issues and higher management cost. In this regard, the ground-penetrating radar (GPR) [25] geophysical inspection tool is featured to be the most viable testing method to ensure a non-intrusive and cost-effective (low acquisition time and use of operators) investigation of the subsurface with minimum disturbance to traffic and, hence, lower driving safety implications.

Fig. 1 – An example of asphalt damage due to the uplift of tree roots at the edge of the lateral lane and at the verge

2. The ground-penetrating radar non-destructive testing method

2.1. Theoretical principles and survey configurations

GPR operates by transmitting electromagnetic (EM) waves towards a surface, typically a soil, and receiving the transmitted or back-reflected signal. The dielectric properties of the medium passed through (i.e., the dielectric permittivity ε, the electric conductivity σ and the magnetic permeability μ) rule the propagation of the EM waves. In more detail, ε and σ have a major influence on the behaviour of the propagating wave, in terms of wave velocity and wave attenuation, respectively, and μ is equal to the free space magnetic permeability μ_0 for all the non-magnetic materials and does not affect the propagation of the EM wave. A GPR system is usually configured by one transmitting and one receiving antenna(s), a control unit, a data storage unit and a display unit. An EM impulse is emitted by the transmitting antenna towards the surface to investigate. Subsequently, the signal is reflected and scattered by the dielectric anomalies/interfaces in the subsurface and collected by a receiving antenna. A conventional analog-to-digital (A/D) converter is used to convert the extracted information in such a way that a real-time displaying of the data as well as additional processing can be performed.

Amongst the advantages of the GPR non-destructive testing (NDT) method, it is worth mentioning the high number of characteristics that can be extracted from the signal (e.g., the time delays, the amplitudes of the reflection peaks and the frequency modulations) in order to estimate the properties of the materials. In addition, ground-coupled or air-coupled antenna configurations can be used depending on the purposes and the types of the investigation. In this regard, the antenna selection is usually driven by a combination of survey parameters, e.g., the required penetration depth, the soil/construction material type and the (expected) size of the targets to detect.

Figure 2 shows a typical cross-section of a flexible pavement structure and the corresponding reflection path from a single GPR measurement, or A-scan. The A-scan provides a punctual "one dimensional" (1-D) information about the configuration of the subsurface structure. Reflections are located in the figure at the electric discontinuities represented by the interfaces of the pavement layers. It is worth noting that the two-way travel time taken by the signal to cover the distance from the transmitter to the receiver (usually given in nanoseconds) is recorded in the vertical axis of an A-scan.
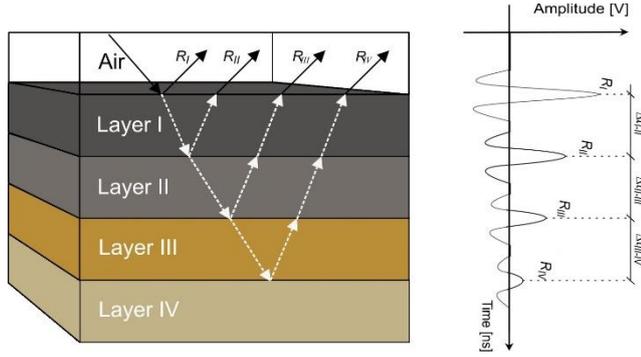
Fig. 2 – Path of EM reflections in a typical cross-section of a road flexible pavement and corresponding A-scan from a single GPR measurement

By knowledge/assumption of the wave propagation velocity in the medium, the collected time can be converted into distance units (usually given in centimetres) in order to display the depth of the signal reflections. The horizontal axis of an A-scan represents the signal amplitude (usually given in Volts). A sequence of A-scans along the scanning line is used to create a "two dimensional" (2-D) matrix called radargram (B-scan). This is typically displayed in real-time for immediate data interpretation purposes. The vertical and horizontal axes of a B-scan represent the two-way travel time/depth information and the distance covered along the scanning line (usually given in meters), respectively.

The C-scan view mode can be developed when a set of B-scans is collected sequentially to cover a certain area and a constant value is taken as a reference along the two-way travel time/depth axis. The C-scan view mode provides a plan view (horizontal 2-D domain) of amplitude maps at specific time/depth of investigation. More insights about visualisation modes can be found in Benedetto et al. [26].

There exists several methods of estimation of the relative dielectric permittivity of the investigated media. Among these, the time-domain signal-picking method [25] relies on the knowledge/assumption of the velocity of propagation v of an EM wave:

$$v = \frac{c}{\sqrt{\varepsilon}} \tag{1}$$

where c is the wave propagation velocity in the free space and ε is the relative dielectric permittivity of the medium passed through. Once the concerning pulse reflections at the layer interfaces are identified (e.g., R_I and R_{II} for Layer I in Figure 1), the travel time between the relevant pulses (e.g., $\Delta t_{I\text{-}II}$ for layer I in Figure 1) can be calculated. If it is considered the two-way travel time path of the signal bouncing back towards the receiving antenna at the (bottom) reflection interface of the layer, then the value of the wave velocity v can be written as follows:

$$v = \frac{2 \times h}{\Delta t} \tag{2}$$

where h is the thickness of the pavement layer. In highway engineering applications, the velocity v is frequently estimated using the thickness h of each layer measured by coring.

Another method used for the estimation of v is the "hyperbola fitting" [27], that relies on the presence of buried localised reflectors or buried cylindrical-shaped objects (e.g., tree roots).

Among the factors affecting the shapes of these hyperbolae, it is worthy of mention the nature of the reflector, the relative permittivity of the surrounding medium as well as the physical conditions of the materials involved.

In the "hyperbola fitting" method, the wave velocity v is proportional to the angle α between the hyperbola asymptotes, in accordance to the following relationship:

$$v = 2 \ tg \ \alpha \tag{3}$$

Several literature studies have proven that v is a function of the vertex coordinates, the object radius and the time delay (e.g., [28, 29]).

Finally, the value of v calculated by Equation (2) and/or Equation (3) can be worked out into Equation (1) in order to evaluate the relative dielectric permittivity ε. Among the processing methods for the estimation of the relative dielectric permittivity, the reflection methods [30] and the volumetric mixing formulae theoretical models [31] have found extensive application in the literature (e.g., [32]).

2.2. Main applications

The first application of GPR can be traced back to the nineteen fifties [33]. The first major historical use was in demining operations [34], whereas nowadays GPR is widely used in a range of disciplines. Among the others, it is worth mentioning the applications in civil and environmental engineering [35], planetary explorations [36], geology [37], archaeology [38], forensic and public safety [39], agricultural and forestry sciences [40, 41].

In the area of forestry science, the first use of GPR can be traced back to 1999 and relates to the mapping of tree root systems [42]. Later GPR applications have focused on the investigation of tree trunks and root systems. In regard to the analysis of tree root systems, the research was mostly related to the assessment of the diameter of roots [43], biomass [44], coarseness [45] and subsurface path in complex urban areas [46]. For the tree trunks investigation, physical and EM factors such as the inner structure of a tree [47, 48], the anisotropy (grain orientation) [49, 50], the moisture level [51] and the frequency of the applied EM field [52] were mostly addressed. Implementation of survey techniques such as using planar [53] or arc [54] perfect electric conductors (PEC) were also carried out. On the other hand, the use of numerical simulation for the interpretation of the geometric properties, physical properties and decays of tree trunks [54] is much more recent.

To the best of the Authors' knowledge, few and very recent studies have focused on the use of GPR for the assessment of the subsurface tree roots' path of street trees. Barone et al. [55] investigated the application of GPR as a forensic geoscience tool for the management of road infrastructures and urban greening. Nichols et al. [56], used GPR to locate and categorise tree roots under urban pavements. The authors performed experimental testing in a laboratory environment and in real-life conditions. Results have proven the viability of GPR in assessing the size and depth of the tree roots. Overlapping of tree roots was found to affect the detectability of these targets.

3. Aim and objective

The aim of this research is to demonstrate the viability of GPR in mapping the subsurface roots path of street trees for the assessment of road safety-critical conditions.

To achieve this Aim, the main objective to pursue is to develop a pilot data processing methodology for a real-time three dimensional (3-D) visualisation of the main features of a street tree root system as well as several visualisation modes (2-D and 3-D domain of investigation) in order to cross-matching effectively all the information available.

4. Methodology

4.1. Equipment and survey methodology

The soil around a 70-year-old fir tree, with a trunk circumference of 3.40 m and an average diameter of 1.10 m, was investigated. A set of 9 circular scans, 0.30 m from one another, were collected all around the tree circumference from 0.50 m the outer surface of the bark (Figure 3). A ground-coupled multi-frequency GPR system equipped with 600 MHz and 1600 MHz central frequency antennas was used for testing purposes. In this regard, a system with antennas coupled to the surface was preferred against air-coupled antenna systems to cover more accurately the investigation area and coping with a relatively complex survey setup. Signals were collected using a time window of 40 ns and steps of 512 samples. The horizontal resolution was set equal to 2.4×10^{-2} m. Only the 600 MHz antenna frequency was considered for data processing purposes.

This frequency was set to reach the maximum penetration depth for detection of the deepest elements of the root system as well as to provide proper resolution of the equipment against critical targets (i.e., roots' dimension with potential damaging capabilities). Therefore, a swept circle area with an outer radius of 3.45 m and an inner radius of 1.05 m was investigated.

4.2. Data processing methodology

A multi-stage data processing methodology is implemented to identify the tree root system under the investigated area. The methodology relies on seven main steps as follows:
1. Signal noise filtering: sequential use of i) the time-zero correction filter, ii) the zero-offset removal and iii) the bandpass filtering is applied to the raw radargrams (2-D domain). In addition, the use of the background removal filters out the unwanted reflections from flat-like layers/interfaces. In this regard, this filter is useful to remove the main reflection from the ground [26]. From now on, the radargrams processed using the above sequence of EM filters will be referred to as "processed radargrams".
2. Target detection: the apices of the tree roots are herein identified by means of the vertices of the hyperbolae that are visualised in the processed radargrams (2-D domain) (Figure 4). It is worth mentioning that the targets detection rate strongly depends on the EM contrast between the tree roots and the surrounding soil. Hence, the detectability highly depends also on the moisture level and compaction of the soil.
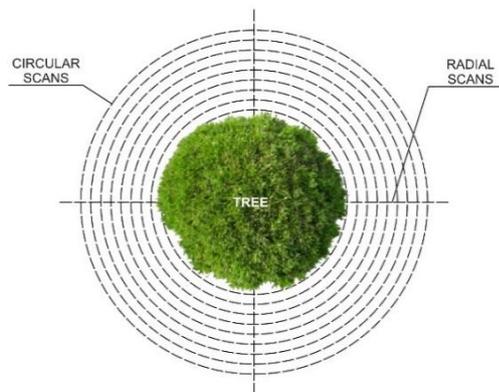

Fig. 3 – Plan view of the circular scans carried out around the investigated tree

3. Target's depth estimation: the depths of the apices detected at stage 2 are here estimated. In this regard, the "hyperbola fitting" method is applied to estimate the velocity of propagation in the soil using Equation (3). Working out this value into Equation (2), it is therefore possible to estimate the depth of the tree roots' apices.
4. Data conversion from Cartesian to polar coordinates: the GPR scans are here converted from the Cartesian to the polar coordinate system (2-D domain). A drawing of this system is shown in Figure 5, where θ is the angle of deviation, r represents the distance from a reference circular scan to the centre of the tree trunk, and z is the depth.
5. Construction of the 3-D domain: a 3-D cylindrical domain with origin at the intersection between the vertical axis of the tree trunk and the ground plane is built.
6. Tracking of the roots: the algorithm follows the identified apices of the tree roots (Stages 2 and 3) within the 3-D cylindrical domain built at stage 5.
7. Path filtering: this stage is dedicated to filter out unnecessary information from stage 6. In-excess paths are identified and removed from the tree root system according to logic-based requirements (e.g., removal of short paths, paths not interconnected to at least one source path, paths not connected with the tree trunk) and signal-noise-based requirements (truncation of low-amplitude data).
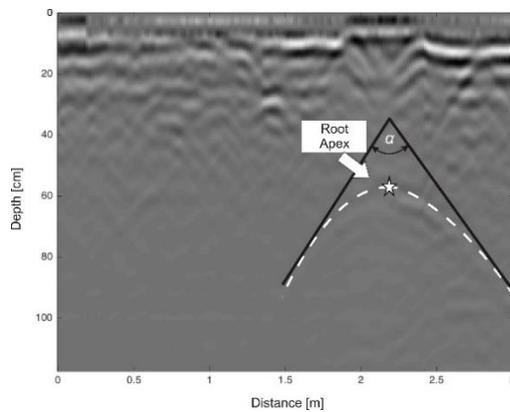

Fig. 4 – Identification of the hyperbola reflection path and corresponding apex (i.e., "Target detection" stage – star-like marker) and angle α between the hyperbola asymptotes (i.e., "Target's depth estimation" stage)
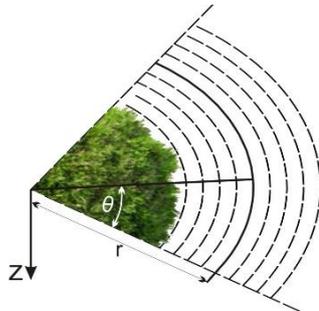

Fig. 5 – Drawing of the polar coordinate system used for data processing purposes (i.e., "Data conversion from Cartesian to polar coordinates" stage)

4. Results and discussion

The collection of concentric radargrams allowed to identify the relevant hyperbolae and locate the in-depth position of the apices (stages 1 to 3 of the data processing scheme). Figure 6 shows an example of a radargram collected along one of the survey rings with a longitudinal development (i.e., circumference) of 6.5 m. Hyperbolic reflection targets can be here observed.

In addition to the identification of these targets, the data conversion step pursued at stage 4 of the data processing scheme along with the 3-D cylindrical domain built at stage 5 allowed for a more comprehensive data interpretation, as several complementary visualisation modes could be used for this purposes. In this regard, tomographic amplitude maps (C-scans) (Figure 7) were developed to provide an in-depth plan view (from $z = 0$ to $z = 1.56$ m) of the distribution of the signal amplitudes over the area of investigation covered. Indeed, high amplitude values were likely indicators to relate to the presence of tree roots. To this effect, the colour map indicates the range of amplitude values, where the red colour identifies areas of high reflectivity that were possibly related to tree root targets.

Finally, the implementation of the multi-stage data processing methodology at stages 6 and 7, allowed to represent the 3-D development of the tree root system underneath the investigated soil (Figure 8). As it can be seen from the figure, the allocation of the roots in a 3-D space is viable for the interpretation of harmful conditions that might create damage to the asphalt surface. The 3-D reconstruction allowed to identify the root system at the pilot scale in terms of orientation, longitudinal development, uplift near the surface and potential early-stage decays.
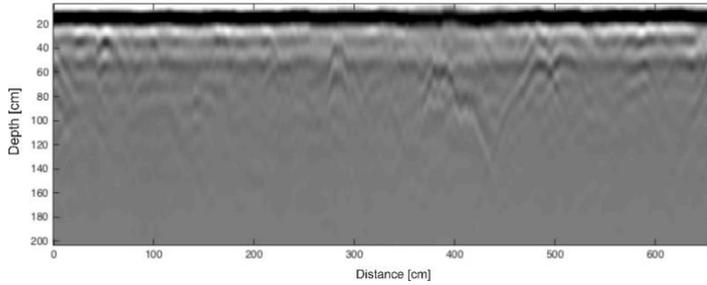

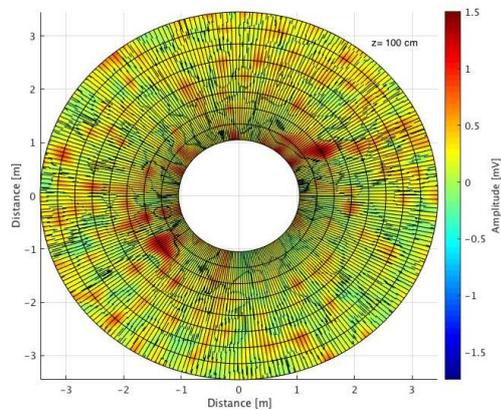Fig. 6 – Radargram collected along a survey ring with a circumference of 6.5 m

Fig. 7 – Tomographic amplitude map extrapolated from the 3-D cylindrical domain at depth z = 100 cm
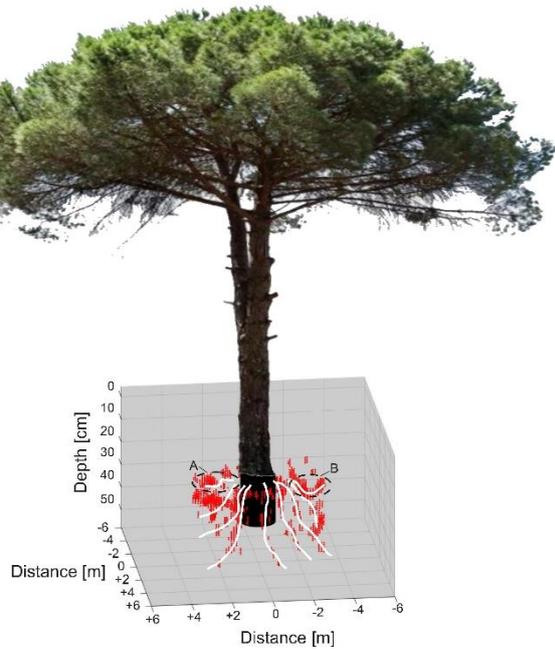
Fig. 8 – 3-D view of the tree root system with potential road safety-critical elements

Overall, the results have proven a root system with a downward roots' orientation, a relatively limited longitudinal development and few uplifts of the roots near the surface. In this regard, two paths were considered as potentially critical to cause asphalt damage (e.g., cracking, unevenness etc.) with road safety implications. In the first case identified (i.e., case A in Figure 8), the downward orientation of the root showed a point of inflection at a limited distance r ($r < 0.5$ m) from the source trunk as well as a shallow peak of uplift potentially harmful to an asphalt surface. In the second case (i.e., case B in Figure 8), the point of inflection was visible at $r \sim 0.5$ m from the source point, whereas the root orientation was directed upward the surface at a relatively long distance from the tree trunk ($r > 1.5$ m).

In addition to the above investigation, the data analysis from the available visualisation modes did not identify decay areas potentially harmful to the overall stability of the tree.

5. Conclusion

This study reports a demonstration of the ground-penetrating radar (GPR) potential in mapping the subsurface roots of street trees for the assessment of road safety-critical conditions. To this purpose, the soil around a 70-year-old fir tree was investigated. A ground-coupled GPR system with central frequency antennas of 600 MHz and 1600 MHz was used for testing purposes.

A pilot multi-stage data processing methodology based on the acquisitions made with the 600 MHz antenna frequency was proposed. The methodology relies on i) the implementation of dedicated signal processing electromagnetic (EM) filters, ii) detection of reflection hyperbolas, iii) location of the apices of the hyperbolae (i.e., root depths), iv) data conversion from Cartesian to polar coordinates, v) construction of a three-dimensional (3-D) domain, vi) tracking of the roots and vii) paths filtering complying with logic-based and signal-noise-based requirements.

In addition, the cross-match of information from different data visualisation modes has proven to aid with the interpretation of the results for detection of potentially harmful (i.e., road-safety critical) situations as well as of areas of structural decay.

Overall, the results have shown a root system with a downward orientation of roots, a relatively limited longitudinal development and few uplifts near the surface. In more detail, two paths were considered as potentially dangerous to create surface damage and, hence, to cause road safety implications. On the contrary, the data analysis from the available visualisation modes did not identify decay areas potentially harmful to the overall stability of the tree. Hence, a limited likelihood was linked with the investigated tree in terms of providing decay to the pavement surface (tree roots uplifting) as well as to fall down (failure of the principal roots).

Future research could task itself to detect further critical features (e.g., roots' mass density, diameter) and provide an enhanced interpretation of the hazard of street tree roots to cause potential damage. In addition, the use of a multi-frequency approach could provide a comprehensive assessment of shallow and deep targets; this could be of paramount importance to raise the detectability of tree roots across the whole depth of interest of a road pavement.

Acknowledgments

References

1. Donovan, G.H., Butry, D.T. (2010). Trees in the city: Valuing street trees in Portland, Oregon. Landscape and Urban Planning, 94(2), pp. 77-83.
2. Donovan, G.H., Butry, D.T., Michael, Y.L., Prestemon, J.P., Liebhold, A.M., Gatziolis, D., Mao, M.Y. (2013). The relationship between trees and human health: evidence from the spread of the emerald ash borer. American Journal of Preventive Medicine, 44(2), pp. 139-145.
3. Mullaney, J., Lucke, T., Trueman, S.J. (2015). A review of benefits and challenges in growing street trees in paved urban environments. Landscape and Urban Planning, 34, pp. 157-166
4. Van Dillen, S.M.E., De Vries, S., Groenewegen, P.P., Spreeuwenberg, P. (2012). Greenspace in urban neighbourhoods and residents health: adding quality to quantity. Journal of Epidemiology and Community Health, 66(6), e8.
5. Kuo, F. E., Sullivan, W. C. (2001). Environment and crime in the inner city: Does vegetation reduce crime? Environment and Behavior, 33, pp. 343–367.
6. Burden, D. (2006). 22 benefits of urban street trees. Retrieved from (www.michigan.gov/documents/dnr/22 benefits 208084 7.pdf).
7. Rhodes, J.R., Ng, C.F., de Villiers, D.L., Preece, H.J., McAlpine, C.A., Possingham, H.P. (2011). Using integrated population modelling to quantify the implications of multiple threatening processes for a rapidly declining population. Biological Conservation, 144, pp. 1081–1088.
8. Vogt, J., Hauer, R.J., Fischer, B.C. (2015). The costs of maintaining and not maintaining the urban forest: a review of the urban forestry and arboriculture literature. Arboricolture & Urban Forestry, 41(6), pp. 293–323.

9. Costello, L.R., McPherson, E.G., Burger, D., Perry, E. J., Kelley, D. (Eds.). (2000–2001). Strategies to reduce infrastructure damage by tree roots. In Proceedings of a symposium for researchers and practitioners International Society of Arboriculture, Western Chapter, Cohasset, CA.
10. Randrup, T.B., McPherson, E.G., Costello, L.R. (2001) A review of tree root conflicts with sidewalks, curbs, and roads. Urban Ecosystems, 5, pp. 209-225.
11. Kirkpatrick, J.B., Davison, A., Daniels, G.D. (2012). Resident attitudes towards trees influence the planting and removal of different types of trees in Australian cities. Landsc Urb Plan, 107, pp. 147–158.
12. Wagar, J.A.,Barker, P.A. (1983). Tree root damage to sidewalk and curbs. J. Arboric. 9, pp. 177–181.
13. McPherson, E.G. (2000) Expenditures associated with conflicts between street tree root growth and hardscape in California, United States. Journal of Arboriculture, 26, pp. 289–297.
14. Sydnor, T.D., Gamstelter, D., Nichols, J., Bishop, B., Favorite, J., Blazer, C., et al. (2000). Trees are not the root of sidewalk problems. Journal of Arboriculture, 26, pp. 20–29.
15. Blunt, S.M. (2008). Trees and pavements- Are they compatible? Arbor J: Int J Urb For, 31, pp. 73–80.
16. Morgenroth, J. (2008). A review of root barrier research. Arbor Urb For, 34, pp. 84-88.
17. Grabosky, J., Hoffner, E., Bassuk, N. (2009). Plant available moisture in stone soil media for use under pavement while allowing urban tree root growth. Arboriculture and Urban Forestry, 35, pp. 271–278.
18. Coder, K. D. (1998). Tree roots and infrastructure damage. Tree root growth control series (March) Georgia: University of Georgia Cooperative Extension Service Forest Resource Publication. FOR98-8.
19. Grabosky, J., Bassuk, N., Marranca, B.Z. (2002). Preliminary findings from measur-ing street tree shoot growth in two skeletal soil installations compared to treelawn plantings. J. Arboric., 28, pp. 106–108.
20. Tighe, S., Li, N., Falls, L.C., Haas, R. (2000). Incorporating road safety into pavement management. Transportation Research Record, 1699, pp. 1–10.
21. Vansauskas, V., Bogdevičius, M. (2009). Investigation into the stability of driving an automobile on the road pavement with ruts, Transport, 24 (2), pp. 170-179.
22. Chan, C.-Y., Huang, B., Yan, X., Richards, S. (2010). Investigating effects of asphalt pavement conditions on traffic accidents in Tennessee based on the pavement management system (PMS), Journal of Advanced Transportation, 44 (3), pp. 150-161.
23. Reynolds, C.C.O., Harris, M.A., Teschke, K., Cripton, P.A., Winters, M., (2009). The impact of transportation infrastructure on bicycling injuries and crashes: A review of the literature, Environmental Health: A Global Access Science Source, 8 (1), pp. 47.
24. Bella, F., Silvestri, M., (2015). Effects of safety measures on driver's speed behavior at pedestrian crossings. Accident Analysis and Prevention, 83, pp. 111-124.
25. Daniels, D.J. (2004). Ground Penetrating Radar, 2nd ed. London: The Institution of Electrical Engineers.
26. Benedetto, A., Tosti, F., Bianchini Ciampoli, L., D'Amico, F. (2017). An overview of ground-penetrating radar signal processing techniques for road inspections. Signal Processing, 132, pp. 201–209.
27. Shihab, S., Al-Nuaimy, W. (2005). Radius estimation for cylindrical objects detected by ground penetrating radar. Subsurface Sensing Technologies and Applications, 6, pp. 151–166.
28. Ristic, A., Petrovacki, D., Govedarica, M. (2009). A new method to simultaneously estimate the radius of a cylindrical object and the wave propagation velocity from GPR data.Comp Geosci35(8),1620–1630.
29. Olhoeft, G. (2000). Maximizing the information return from ground penetrating radar, Journal of Applied Geophysics, 43, pp. 175–187.
30. Redman, J., Davis, J., Galagedara, L., Parkin, G. (2002). Field studies of GPR air launched surface reflectivity measurements of soil water content. In: Proceedings of the 9th international conference on ground penetrating radar (GPR 2002), Santa Barbara, California, USA; 2002. pp. 156–61. art. no. 4758.
31. Birchak, J.R., Gardner, C.G., Hipp, J.E., Victor, J.M. (1974). High dielectric constant microwave probes for sensing soil moisture. Proc IEEE, 62, pp. 93–102.
32. Tosti, F., Bianchini Ciampoli, L., Calvi, A., Alani, A.M., Benedetto, A. (2018). An investigation into the railway ballast dielectric properties using different GPR antennas and frequency systems. NDT and E International, 93, pp. 131-140.
33. El Said, M. (1956). Geophysical prospection of underground water in the desert by means of electromagnetic interference fringes, in Proc. I.R.E., 44, pp. 24–30.

34. Potin, D., Duflos, E., Vanheeghe, P. (2006). Landmines ground-penetrating radar signal enhancement by digital filtering, IEEE Transactions on Geoscience and Remote Sensing, 44 (9), pp. 2393-2406.
35. Benedetto, A., Pajewski, L. (2015). Civil Engineering Applications of Ground Penetrating Radar. Springer Transactions in Civil and Environmental Engineering Book Series.
36. Tosti, F., Pajewski, L. (2015). Applications of radar systems in Planetary Sciences: an overview Chapt. 15 - Civil Engineering Applications of Ground Penetrating Radar, Springer Transactions in Civil and Environmental Engineering Book Series, pp. 361–371.
37. Benson, A.K. (2001). Applications of ground penetrating radar in assessing some geological hazards: examples of groundwater contamination, faults, cavities," J App Geophys, 33 (1-3), pp. 177–193.
38. Goodman, D. (1994). Ground-penetrating radar simulation in engineering and archaeology, Geophysics, 59 (2), pp. 224-232.
39. Schultz, J.J., Collins, M.E., Falsetti, A.B. (2006). Sequential monitoring of burials containing large pig cadavers using ground-penetrating radar," Journal of Forensic Sciences, 3, pp. 607-616.
40. Lambot, S., Weihermüller, L., Huisman, J.A., Vereecken, H., Vanclooster, M., Slob, E.C. (2006). Analysis of air-launched ground-penetrating radar techniques to measure the soil surface water content. Water Resources Research 42(11): W11403.
41. Butnor, J.R., Doolittle, J.A., Kress, L., Cohen, S., Johnsen, K.H. (2001). Use of ground-penetrating radar to study tree roots in the southeastern United States. Tree Physiology, 21 (17), pp. 1269-1278.
42. Hruska, J., Cermák, J., Sustek, S. (1999). Mapping tree root systems with ground-penetrating radar. Tree Physiology, 19 (2), pp. 125-130.
43. Barton, C.V.M., Montagu, K.D. Detection of tree roots and determination of root diameters by ground penetrating radar under optimal conditions (2004) Tree Physiology, 24 (12): 1323-1331.
44. Butnor, J.R., Doolittle, J.A., Johnsen, K.H., Samuelson, L., Stokes, T., Kress, L. Utility of ground-penetrating radar as a root biomass survey tool in forest systems (2003)Soil Sci S Ame J,67(5):1607-15.
45. Guo, L., Chen, J., Cui, X., Fan, B., Lin, H. Application of ground penetrating radar for coarse root detection and quantification: A review (2013) Plant and Soil, 362 (1-2), pp. 1-23.
46. Stokes, A., Fourcaud, T., Hruska, J., Cermak, J., Nadyezdhina, N., Nadyezhdin, V., Praus, L. An evaluation of different methods to investigate root system architecture of urban trees in situ: I. ground-penetrating radar (2002) Journal of Arboriculture, 28 (1): pp. 2-10.
47. Nicolotti G., Socco L.V., Martinis R., Godio A., Sambuelli L., 2003. Application and comparison of three tomographic techniques for detection decay in trees, Journal of Arboriculture, 29 (2), pp. 66–78.
48. Butnor, J.R., Pruyn, M.L., Shaw, D.C., Harmon, M.E., Mucciardi, A.N., Ryan, M.G. (2009). Detecting defects in conifers with ground penetrating radar: applications and challenges, For Path,39(5),309–322.
49. Rodríguez-Abad, I., Martínez-Sala, R., García-García, F., Capuz-Lladro, R. (2010). Nondestructive methodologies for the evaluation of moisture content in sawn timber structures: ground-penetrating radar and ultrasound techniques, Near Surface Geophysics 8, pp. 475–482.
50. Martínez-Sala, R., Rodríguez-Abad, I., Diez Barra, R., Capuz-Lladró, R. (2013). Assessment of the dielectric anisotropy in timber using the nondestructive GPR technique, Constr Build Mat, 38, 903–911.
51. Rodríguez-Abad, I., Martínez-Sala, R., Capuz Lladró, R., Díez Barra, R., García-García, F. (2011). Assessment of the variation of the moisture content in the pinus pinaster Ait using the non destructive GPR technique, Materiales de Construcción, 61 (301), pp. 143–156.
52. Sahin, H., Ay, N. (2004). Dielectric properties of hardwood species at microwave frequencies, Journal of Wood Science, 50 (4), pp. 375–380.
53. Lorenzo, H., Pérez-Gracia, V., Novo, A., Armesto, J. (2010). Forestry applications of ground-penetrating radar, Forest Systems, 19 (1), pp. 5–17.
54. Ježová, J., Mertens, L., Lambot, S. (2016). Ground-penetrating radar for observing tree trunks and other cylindrical objects, Construction and Building Materials, 123, pp. 214-225.
55. Barone, P.M., Ferrara, C., Di Maggio, R.M., Salvati, L. (2016). When the crime scene is the road: forensic geoscienceindicators applied to road infrastructure and urban greening. Geosciences. 6 (50).
56. Nichols, P., McCallum, A., Lucke T. (2017). Using ground penetrating radar to locate and categorise tree roots under urban pavements. Forestry and Urban Greening, http://dx.doi.org/doi:10.1016/j.ufug.2017.06.019